

Stability of Symmetric Solitary Wave Solutions of a Forced Korteweg-de Vries Equation and the Polynomial Chaos

Hongjoong Kim^{1,*} and Kyoung-Sook Moon²

¹ Department of Mathematics, Korea University, Seoul 136-701, Korea

² Mathematics & Information, Gachon University, Gyeonggi-do 461-701, Korea

Revised 19 June 2012; Accepted (in revised version) 25 June 2012

Available online 9 November 2012

Abstract. In this paper, we consider the numerical stability of gravity-capillary waves generated by a localized pressure in water of finite depth based on the forced Korteweg-de Vries (FKdV) framework and the polynomial chaos. The stability studies are focused on the symmetric solitary wave for the subcritical flow with the Bond number greater than one third. When its steady symmetric solitary-wave-like solutions are randomly perturbed, the evolutions of some waves show stability in time regardless of the randomness while other waves produce unstable fluctuations. By representing the perturbation with a random variable, the governing FKdV equation is interpreted as a stochastic equation. The polynomial chaos expansion of the random solution has been used for the study of stability in two ways. First it allows us to identify the stable solution of the stochastic governing equation. Secondly it is used to construct upper and lower bounding surfaces for unstable solutions, which encompass the fluctuations of waves.

AMS subject classifications: 65C20, 65C30

Key words: Stability, solitary waves, polynomial chaos, forced Korteweg-de Vries equation.

1 Introduction

We investigate two-dimensional gravity-capillary waves in this paper. The analysis of properties of those waves such as the stability analysis has been one of main research areas in fluid mechanics, see [1–6] and the references therein. The Froude number F and the Bond number τ are important variables for the description of those waves. When F is close to unity and $\tau > 1/3$, the gravity-capillary waves can be modeled by the Korteweg-de Vries (KdV)-type equations. When the waves are generated by a

*Corresponding author.

Email: hongjoong@korea.ac.kr (H. Kim), ksmoon@gachon.ac.kr (K. Moon)

localized pressure distribution or when the interfacial waves are considered in a spatial domain with bumps, forced KdV-type equations can be derived. Shen et al. in [7] derived a forced Korteweg-de Vries (FKdV) equation asymptotically. They found symmetric steady-state solitary-wave-like solutions and studied their stabilities. Choi et al. extended the study to derive a forced modified Korteweg-de Vries (FMKdV) equation in [8] and found symmetric steady-state solutions. The stability analysis of a damped KdV equation in a quarter plane was performed by Bona et al. in [9]. Larkin performed a mathematical analysis in [10] to prove the existence and uniqueness of strong and weak global solutions for the FMKdV equation in a bounded domain, and Pava and Natali [11] studied periodic traveling wave solutions for the critical KdV equation. Camassa and Wu [12, 13] performed the analysis of the stability for steady solitary-wave solutions and confirmed their analytical findings with accurate numerical computations. Grimshaw et al. [14] also performed the stability analysis on two-dimensional localized solitary waves from the steady forced KdV equation. Recently Chardard et al. derived solutions of the stationary forced KdV equation in [15] and Kim et al. computed the solutions of the forced modified KdV equation in [16].

Maleewong et al. derived the forced Korteweg-de Vries equation (2.1) in Section 2 in [17] and performed a stability analysis in [14]. In this study, we observe the evolutions of the solutions from this equation by perturbing its time-independent symmetric solitary-wave-like solutions. Our computation found four depression and one elevation time-independent solutions as Grimshaw et al. did in [14] and the simulation results show that the evolutions of the solution waves in time are dependent upon the magnitude of the perturbation. Thus, we regard the perturbation as a random variable in this study and we interpret the resultant governing equation as a stochastic differential equation. In this paper, we try to answer following two questions. First, is it possible to identify the stable solution, if it exists, among several time-independent solutions? Secondly, is it possible to estimate the magnitudes of the fluctuations of unstable solutions? Due to the random perturbation in the governing equation, the solution is a function of the deterministic and random variables. Cameron and Martin [18] proved that such a solution can be separated into deterministic and random variables by a Fourier series with respect to a certain polynomial chaos. Mikulevicius and Rozovskii considered problems with a random variable following a Brownian motion and performed theoretical analysis with respect to the polynomial chaos based on the Hermite polynomials in [19, 20]. Ghanem and Spanos extended the study of the Gaussian stochastic process and the Hermite polynomial chaos to uncertainty problems in solid mechanics in [21, 22]. Xiu and Karniadakis [23] showed that optimal polynomial chaos is different when the distributions of the random variable is changed. For instance, the Hermite polynomial is optimal for the Gaussian random variable while the Laguerre polynomials is optimal for the Gamma random variable. Askey and Wilson classified the hypergeometric orthogonal polynomials for various types of random distributions and presented their properties in [24].

We derive a numerical algorithm for the forced Korteweg-de Vries equation. This research extends those of Grimshaw et al. [14] and Kim et al. [16], and the random

variable is assumed to be a uniform random variable for simplicity. In Section 2, steady waves are considered. The numerical scheme for the stochastic differential equation based on the polynomial chaos is introduced in Section 3. Simulation results are shown in Section 4.

2 Steady state solutions

Two-dimensional gravity-capillary waves having a speed U in water of depth h can be described by the forced Korteweg-de Vries equation

$$2\eta_t + (F^2 - 1)\eta_x - \frac{3}{2}(\eta^2)_x + \left(\tau - \frac{1}{3}\right)\eta_{xxx} = F^2 p_x(x), \quad (2.1)$$

when the Froude number $F = U/\sqrt{gh} < 1$ and the Bond number $\tau = T/\rho gh^2$ dominates, $\tau > 1/3$ as Maleewong et al. showed in [17]. $F = 0.9$ and $\tau = 0.4$, respectively, in this study. T is the coefficient of surface tension, g is the gravity acceleration and ρ represents the water density. $p(x) = \epsilon \operatorname{sech}^2(x)$ describes the localized pressure distribution, where ϵ is the magnitude of the pressure. We investigate the evolutions of the time-independent symmetric solitary-wave-like solutions of (2.1). A shooting method with a matching process has been used to find steady symmetric solitary-wave-like solutions as Choi et al. did in [8]. As in [14], we found five symmetric steady solitary-wave-like solutions for $F = 0.9$ and $\tau = 0.4$: two depression waves I and II in Fig. 1 (Left) with $\epsilon = -0.01$, two more depression waves III and IV with $\epsilon = 0.01$, and one elevation wave V in Fig. 1 (Right) with $\epsilon = -0.01$. Eq. (2.1) is solved with the perturbed steady solution

$$\eta_0(x) = (1 + \zeta)\eta^s(x), \quad (2.2)$$

as the initial condition. $\eta^s(x)$ represents steady solutions I-V in Fig. 1 and ζ is a perturbation. Eq. (2.1) is solved with a small ζ , $-0.1 \leq \zeta \leq 0.1$ in Section 4.1, and with a moderate ζ , $-0.5 \leq \zeta \leq 0.5$ in Section 4.2.

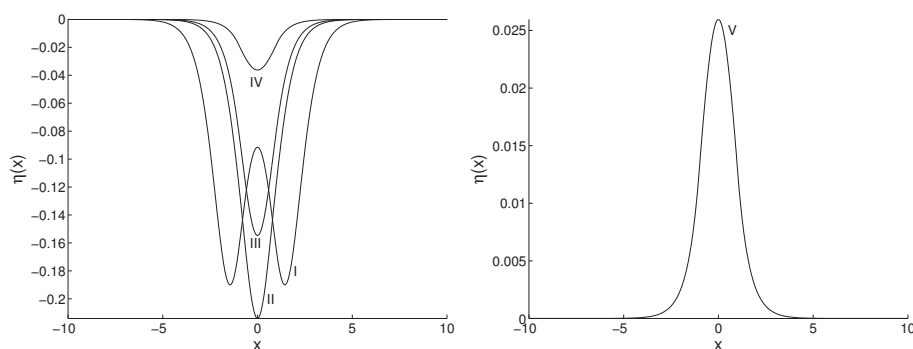


Figure 1: Time-independent symmetric solitary-wave-like solutions of (2.1) when $F = 0.9$ and $\tau = 0.4$. (Left) Four depression waves with $\epsilon = -0.01$ for I and II and $\epsilon = 0.01$ for III and IV and (Right) one elevation wave V with $\epsilon = -0.01$.

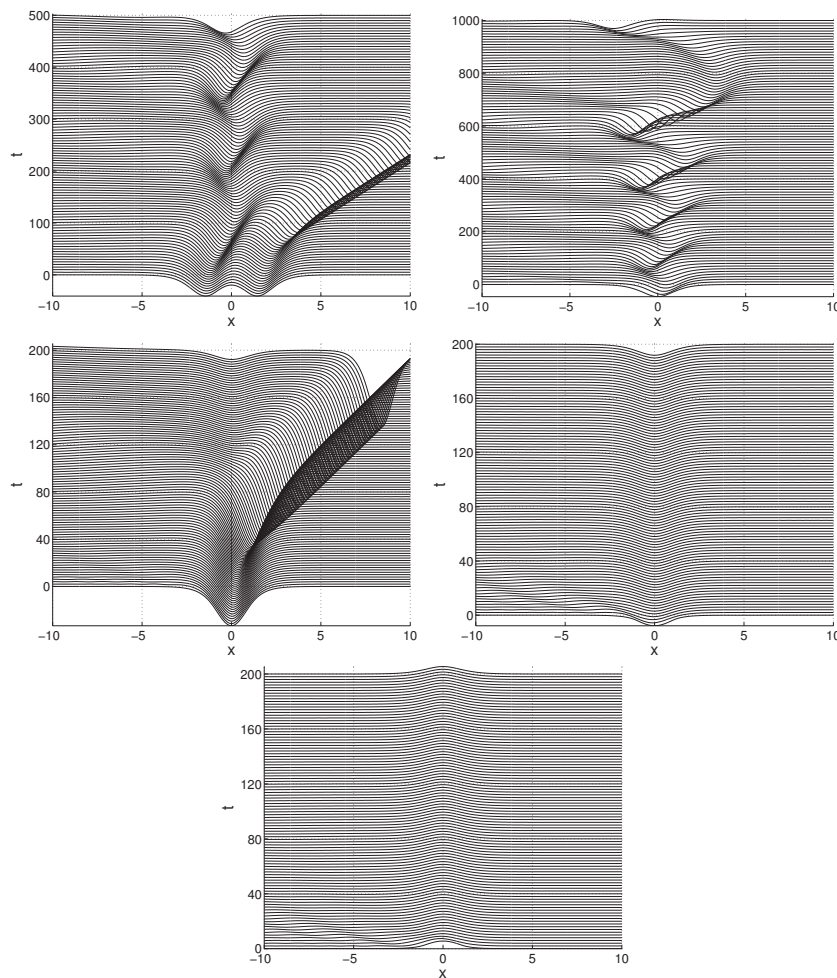


Figure 2: Time evolutions of 5 waves in Fig. 1 from the forced KdV equation (2.1) and the initial condition (2.2) with perturbation $\zeta = 0.075$. Top: Depression waves I and II from $\epsilon = -0.01$, Middle: Depression waves III and IV from $\epsilon = 0.01$, Bottom: Elevation wave V from $\epsilon = -0.01$.

Fig. 2 shows the time evolutions of the time-independent symmetric solitary-wave-like solution waves of (2.1) and (2.2) when the perturbation $\zeta = 0.075$. It manifests that waves I, II, III are not stable in time and on the other hand the waves IV and V are stable. Kim et al. considered the evolutions of the depression waves I-IV in time in [16] for one value $\zeta = 0.1$ only and concluded that the wave IV is the only stable solution among those 4 depression waves. Before we accept the claim by Kim et al. [16] regarding the stability of the wave IV, we want to question if there is any effect from the perturbation. Thus, we vary the values of the perturbation and observe the corresponding evolutions.

Fig. 3 compares the evolutions of the depression wave I from (2.1) and (2.2) when the perturbation ζ takes values of (from the top left)

$$\zeta = -0.075, -0.05, -0.025, 0.025, 0.05, 0.075. \quad (2.3)$$

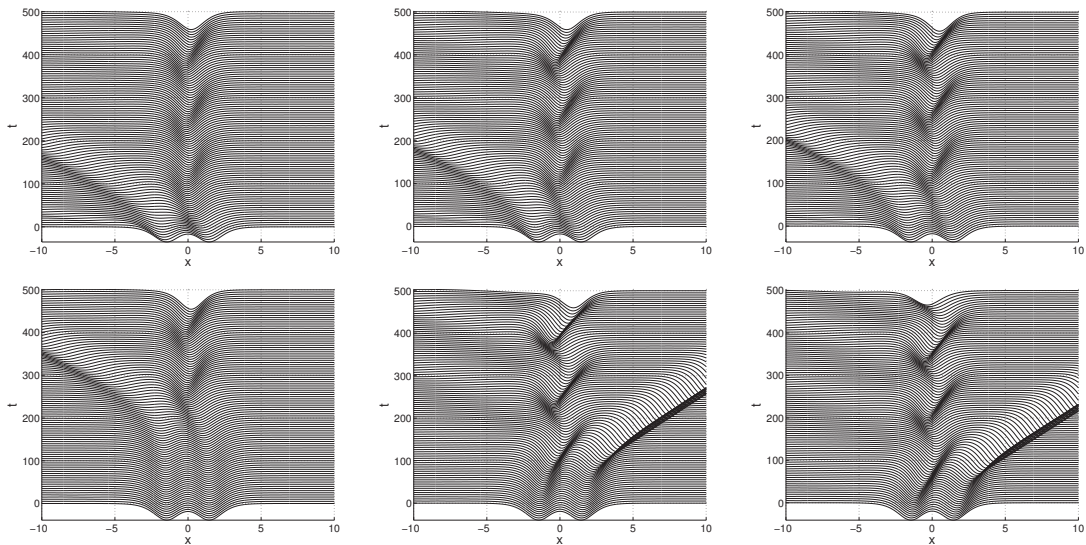


Figure 3: Time evolutions of the depression wave I from (2.1) and (2.2) with $\epsilon = -0.01$ when the perturbation ζ takes values in (2.3) (from the top left).

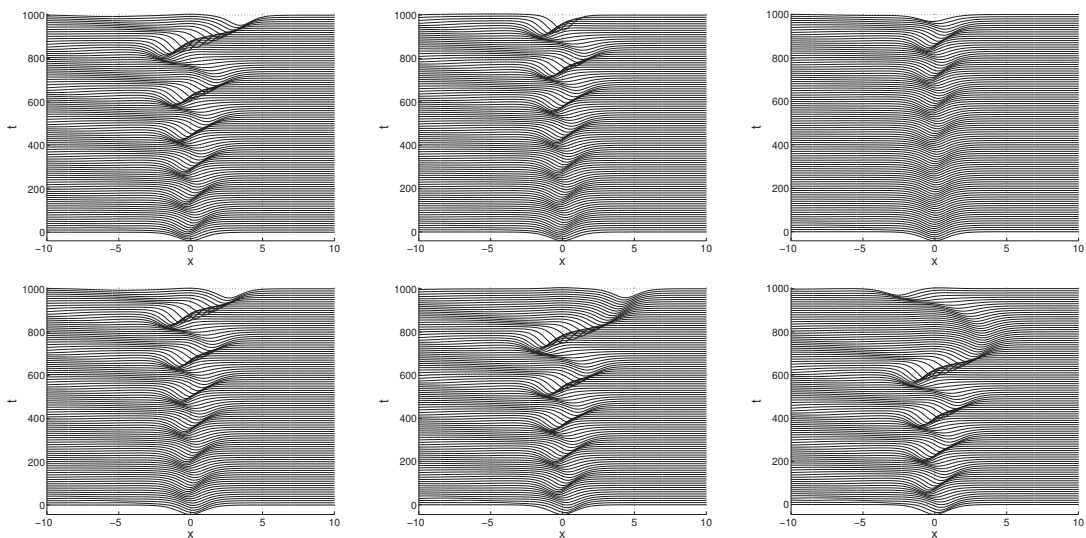


Figure 4: Time evolutions of the depression wave II from (2.1) and (2.2) with $\epsilon = -0.01$ when the perturbation ζ takes values in (2.3) (from the top left).

Fig. 4 compares those for the depression wave II. Fig. 3 and Fig. 4 show that characteristics of the evolutions are affected by the magnitudes of the perturbation ζ and that we need more in-depth analysis upon the effect of the perturbation on the stability.

3 Stochastic differential equation

Numerical simulations in Section 2 show that the value of the perturbation changes the properties of the evolutions of the waves of (2.1). Thus, let us assume that the per-

turbation ξ is a random variable. Then the two-dimensional capillary-gravity equation is governed by a stochastic differential equation, that is, the forced Korteweg-de Vries equation (2.1) with a random initial condition (2.2). There are several numerical approaches for stochastic differential equations. One is the Monte Carlo method, which generates realizations of the random variable and solves the given equation for each realization. Since the number of realizations should be sufficiently large for the Monte Carlo method, its computational cost is usually expensive. Polynomial chaos expansion is another approach for the stochastic differential equation. This method expands the stochastic solution as a Fourier series with respect to certain polynomials $\{J_n(x)\}$. These polynomials are chosen so that they are orthonormal when the inner product is defined by

$$\langle J_m, J_n \rangle \equiv \int_I J_m(x) J_n(x) d\mu = \delta_{mn},$$

where the measure μ is expressed by $d\mu(x) = w(x)dx$ for the probability density function $w(x)$ for the random variable and I is the support of $w(x)$. Kim performed a preliminary analysis in [25] on the polynomial chaos based on the Hermite polynomials when the random variable follows the Gaussian distribution. Since the perturbation ξ follows the uniform distribution in this study, let us apply the Legendre polynomials following the Askey's classification [24].

Let $J_n^*(x)$ represent Legendre polynomials of degree n defined by

$$J_n^*(x) = \frac{(-1)^n}{2^n n!} \frac{d^n}{dx^n} ((1-x)^n (1+x)^n)$$

with $J_0^*(x) = 1$. For instance,

$$J_1^*(x) = x, \quad J_2^*(x) = \frac{3x^2 - 1}{2}, \quad J_3^*(x) = \frac{5x^3 - 3x}{2}.$$

The polynomials $\{J_n^*(x)\}$ satisfy a recurrence relation,

$$xJ_n^*(x) = \frac{n+1}{2n+1} J_{n+1}^*(x) + \frac{n}{2n+1} J_{n-1}^*(x), \quad (3.1)$$

for $n = 1, 2, 3, \dots$. Legendre polynomials $\{J_n^*(x)\}$ are orthogonal when the inner product is defined by

$$\langle J_m^*, J_n^* \rangle \equiv \int_I J_m^*(x) J_n^*(x) d\mu,$$

where the measure μ is expressed by $d\mu(x) = w(x)dx$, using the probability density function of the uniform distribution $w(x) = 1/2$ with the support $I = [-1, 1]$. The normalized Legendre polynomials $\{J_n(x)\}$,

$$J_n(x) = \frac{1}{\sqrt{\langle J_n^*, J_n^* \rangle}} J_n^*(x)$$

are then orthonormal,

$$\langle J_m^*, J_n^* \rangle = \delta_{mn}.$$

See [26] for more information on orthogonal polynomials. Let \mathbb{I} denote the set of multi-indices with finitely many non-zero components,

$$\mathbb{I} = \left\{ \alpha = (\alpha_1, \alpha_2, \dots) \mid \alpha_i \in \{0, 1, 2, \dots\}, \quad |\alpha| \equiv \sum_{i=1}^{\infty} \alpha_i < \infty \right\}.$$

We express the solution η of (2.1) as the Fourier series with respect to the normalized Legendre polynomials

$$\eta(x, t, \xi) = \sum_{\alpha \in \mathbb{I}} \eta_{\alpha}(x, t) J_{\alpha}(\xi),$$

where η_{α} represents the Fourier coefficients $\eta_{\alpha} = E[\eta(x, t, \xi) J_{\alpha}(\xi)]$ with respect to $J_{\alpha}(\xi) = \prod_{i=1}^{\infty} J_{\alpha_i}(\xi_i)$ for each multi-index $\alpha = (\alpha_1, \alpha_2, \dots)$ and the normalized Legendre polynomials $J_{\alpha_i}(\xi_i)$. This polynomial chaos separates the deterministic variables η_{α} and random variables $J_{\alpha}(\xi)$ from the solution $\eta(x, t, \xi)$. When the multi-index α is expanded, η can be written as

$$\begin{aligned} \eta(x, t, \xi) = & \hat{\eta}_0 J_0 + \sum_{i=1}^{\infty} \hat{\eta}_i J_1(\xi_i) + \sum_{i=1}^{\infty} \sum_{j=1}^i \hat{\eta}_{ij} J_2(\xi_i, \xi_j) \\ & + \sum_{i=1}^{\infty} \sum_{j=1}^i \sum_{k=1}^j \hat{\eta}_{ijk} J_3(\xi_i, \xi_j, \xi_k) + \dots, \end{aligned} \quad (3.2)$$

where $J_n(\xi_1, \xi_2, \dots, \xi_n)$ denotes the polynomial chaos of order n in the n independent and identically distributed random variables $\xi = (\xi_1, \xi_2, \dots, \xi_n)$. For notational simplicity, we adopt the notation of Xiu and Karniadakis [23] to express (3.2) as

$$\eta(x, t, \xi) = \sum_{\alpha=0}^{\infty} \eta_{\alpha} J_{\alpha}(\xi). \quad (3.3)$$

Note that there is a one-to-one correspondence between the functions $J_n(\xi_1, \xi_2, \dots, \xi_n)$ in (3.2) and $J_{\alpha}(\xi)$ in (3.3) and also between $\hat{\eta}_{1,2,\dots,n}$ and η_{α} . When this expansion (3.3) replaces η in (2.1), the Eq. (2.1) can be written as

$$\begin{aligned} 2 \left(\sum_{\alpha=0}^{\infty} \eta_{\alpha} J_{\alpha} \right)_t + (F^2 - 1) \left(\sum_{\alpha=0}^{\infty} \eta_{\alpha} J_{\alpha} \right)_x - 3 \left(\sum_{\beta=0}^{\infty} \eta_{\beta} J_{\beta} \right) \left(\sum_{\gamma=0}^{\infty} \eta_{\gamma} J_{\gamma} \right)_x \\ + \left(\tau - \frac{1}{3} \right) \left(\sum_{\alpha=0}^{\infty} \eta_{\alpha} J_{\alpha} \right)_{xxx} = F^2 \left(\sum_{\alpha=0}^{\infty} p_{\alpha} J_{\alpha} \right)_x, \end{aligned} \quad (3.4)$$

where p_{α} is the Fourier coefficient of p with respect to $J_{\alpha}(\xi)$. Since J_{α} 's are an orthonormal basis, we can derive a system of equations for η_{α} 's,

$$2(\eta_{\alpha})_t + (F^2 - 1)(\eta_{\alpha})_x - 3 \sum_{\beta, \gamma=0}^{\infty} e_{\alpha\beta\gamma} \eta_{\beta} (\eta_{\gamma})_x + \left(\tau - \frac{1}{3} \right) (\eta_{\alpha})_{xxx} - F^2 (p_{\alpha})_x = 0,$$

where $e_{\alpha\beta\gamma} = \int_I J_\alpha(x) J_\beta(x) J_\gamma(x) w(x) dx$. When this infinite system is truncated into a finite P -dimension,

$$2(\eta_\alpha)_t + (F^2 - 1)(\eta_\alpha)_x - 3 \sum_{\beta, \gamma=0}^P e_{\alpha\beta\gamma} \eta_\beta (\eta_\gamma)_x + \left(\tau - \frac{1}{3}\right) (\eta_\alpha)_{xxx} - F^2 (p_\alpha)_x = 0, \quad (3.5)$$

we obtain the system for the P^{th} order polynomial chaos,

$$\eta(x, t, \xi) = \sum_{\alpha=0}^P \eta_\alpha J_\alpha(\xi). \quad (3.6)$$

Since the solution of the stochastic differential equation (2.1) is random, one is interested in the statistical moments of the solution instead of the solution corresponding to a specific realization of the random variable. Since the Legendre polynomials are orthonormal, we can easily prove that the mean of $\eta(x, t, \xi)$ is

$$E[\eta(x, t, \xi)] = \eta_0(x, t) \quad (3.7)$$

and that the second moment is

$$E[\eta^2(x, t, \xi)] = \sum_{\alpha} \eta_\alpha^2(x, t).$$

Thus, the variance is obtained by

$$\text{Var}[\eta(x, t, \xi)] = \sum_{\alpha \neq 0} \eta_\alpha^2(x, t). \quad (3.8)$$

Note that those statistical moments can be derived from the numerical solutions of the system of Eqs. (3.5) and since the system is deterministic, the system (3.5) needs to be solved only once. Thus, it is anticipated that the computational cost will not be expensive with the polynomial chaos expansion.

4 Numerical simulations

We consider the forced Korteweg-de Vries equation (2.1),

$$2\eta_t + (F^2 - 1)\eta_x - \frac{3}{2}(\eta^2)_x + \left(\tau - \frac{1}{3}\right)\eta_{xxx} = F^2 p_x(x)$$

with the initial condition (2.2),

$$\eta_0(x) = (1 + \xi)\eta^s(x),$$

where ξ is a uniform random variable. The steady solution $\eta^s(x)$ is perturbed by a small amount in Section 4.1 and by a moderate amount in Section 4.2. The Fourier spectral method [27] is used for the spatial differentiation of the system of Eqs. (3.5) for the polynomial chaos (3.6), and the resultant differential equations in time are solved using the fourth order Runge Kutta method.

4.1 FKdV equation with a small perturbation

In this section, the forced KdV equation (2.1) is solved when the steady solution is initially perturbed by up to 10% and ξ follows a uniform distribution over the interval $[-0.1, 0.1]$.

Fig. 5 shows the mean $E[\eta(x, t, \xi)]$ of η in time and space for five symmetric steady state waves I-V. The depression waves I and II for $\epsilon = -0.01$ are expected to be separated into several waves, while the depression wave III for $\epsilon = 0.01$ generates traveling solitary waves leaving behind the steady solitary wave. Grimshaw et al. presented similar results in [14]. Figures for the depression waves I, II, III illustrate that those three solution waves are expected to fluctuate in time, implying that they are not stable, while the figures for the depression wave IV and the elevation wave V show that their means do not change in time.

Fig. 6 shows the variances $Var[\eta(x, t, \xi)]$. Figures for the depression waves I, II, III show the variances of their random fluctuations and justify the expectation that these waves are unstable in time. The figures for the depression wave IV and the elevation

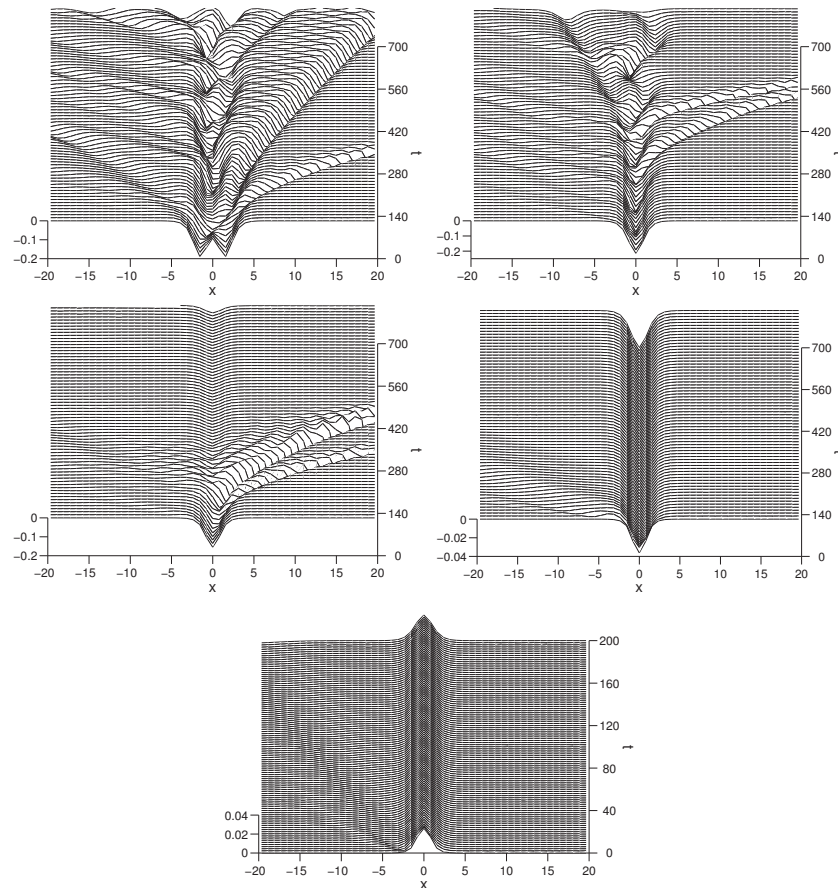


Figure 5: Means of η from (2.1) and (2.2) in time and space. Top: Depression waves I and II from $\epsilon = -0.01$, Middle: Depression waves III and IV from $\epsilon = 0.01$, Bottom: Elevation wave V from $\epsilon = -0.01$.

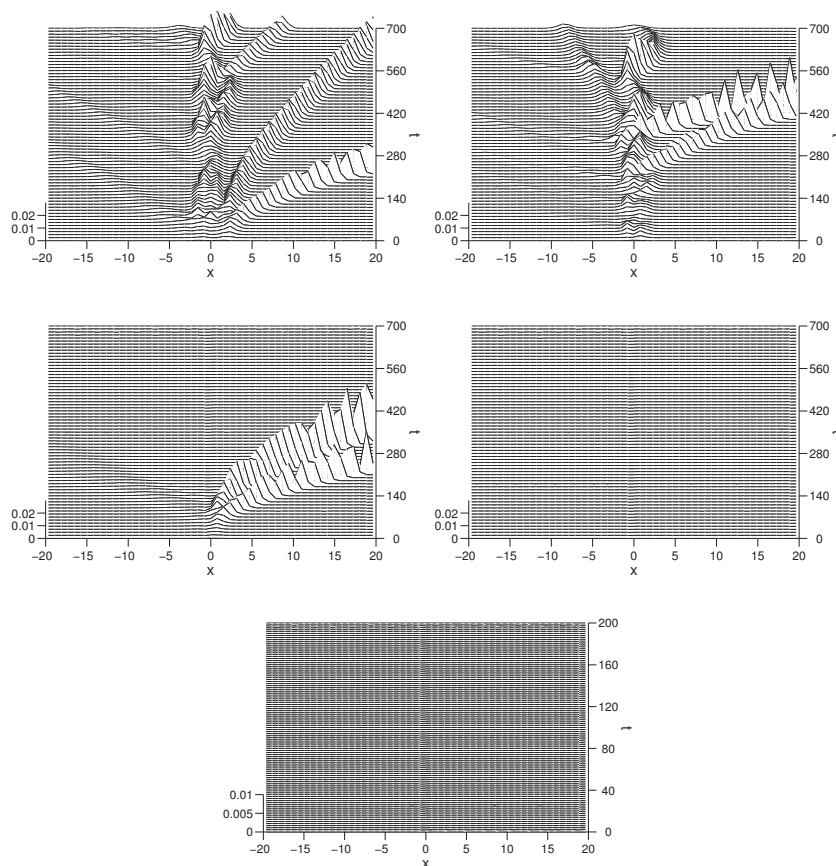


Figure 6: Variances of η from (2.1) and (2.2) in time and space. Top: Depression waves I and II from $\epsilon = -0.01$, Middle: Depression waves III and IV from $\epsilon = 0.01$, Bottom: Elevation wave V from $\epsilon = -0.01$.

wave V show on the other hand that their variances are zero in time. This implies that the wave IV at each time is identical to its mean and the wave V is identical to its mean, respectively. Since Fig. 5 shows that the means for waves IV and V do not change in time, we can conclude that the waves IV and V themselves do not change in time. Combining the results in Fig. 5 and Fig. 6, the polynomial chaos allows us to identify two stable symmetric solitary-wave-like solution of (2.1), that is, the depression wave IV and the elevation wave V.

Those unstable waves I, II, III produce random fluctuations during their propagations and the polynomial chaos can be used to estimate these instabilities as shown below. Since the variance is a measure of how far realizations of a random variable are spread out about its mean, we may construct surfaces,

$$[\text{mean} - \sigma \text{ standard deviation}, \text{mean} + \sigma \text{ standard deviation}] \quad (4.1)$$

with a parameter σ . At each time, these surfaces define two curves in space, which may be used to estimate fluctuations of the unstable waves I, II, III. Fig. 7 (Top Left) shows the fluctuations for the depression wave I from (2.1) and (2.2) with $\epsilon = -0.01$

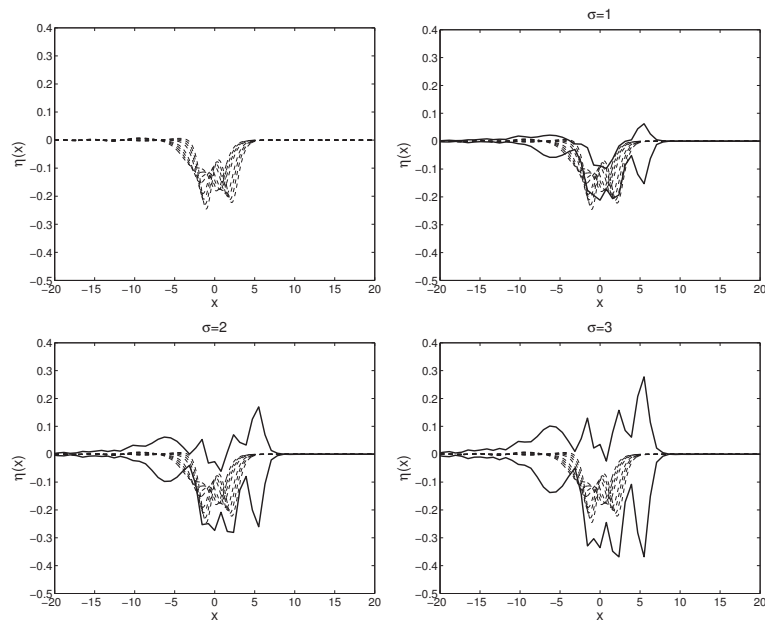


Figure 7: (Top Left) Fluctuations of the depression wave I from (2.1) and (2.2) with $\epsilon = -0.01$ for ξ values in (2.3) at $t = 100$ and (Top Right) those with the curves (4.1) for $\sigma = 1$. (Bottom) Fluctuations with the curves (4.1) for $\sigma = 2$ and $\sigma = 3$.

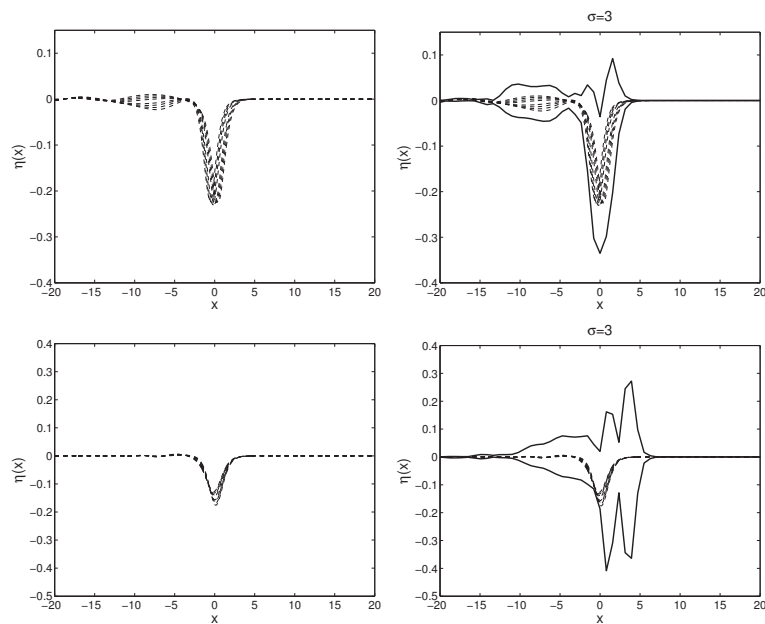


Figure 8: (Top Left) Fluctuations of the depression wave II from (2.1) and (2.2) with $\epsilon = -0.01$ for ξ values in (2.3) at $t = 100$ and (Top Right) those with the curves (4.1) for $\sigma = 3$. (Bottom Left) Fluctuations of the depression wave III from (2.1) and (2.2) with $\epsilon = 0.01$ for ξ values in (2.3) at $t = 100$ and (Bottom Right) those with the curves (4.1) for $\sigma = 3$.

for ζ values in (2.3) at $t = 100$ and Fig. 7 (Top Right) shows those fluctuations together with the proposed curves (4.1) for $\sigma = 1$. Two figures in Fig. 7 (Bottom) show the curves for $\sigma = 2$ and $\sigma = 3$. The figure shows that the fluctuations are encompassed sufficiently well by the given curves (4.1) when σ is 3. Fig. 8 shows the results for the other unstable depression waves II and III, respectively. Simulation results show that the proposed curves encompass random fluctuations of unstable waves and thus the polynomial chaos framework can be used to measure the instabilities of unstable solutions.

4.2 FKdV equation with a moderate perturbation

In this section the forced Korteweg-de Vries equation (2.1) is solved with the initial condition (2.2), where a uniform random variable ζ ranges between -0.5 and 0.5. That is, the steady solution is initially perturbed by up to 50%. Fig. 9 shows the means $E[\eta(x, t, \zeta)]$ of η and Fig. 10 shows the variances $Var[\eta(x, t, \zeta)]$. Based on the same analysis as in Section 4.1, waves IV and V are stable while waves I, II, III are unstable. As in Section 4.1 for a small ζ , Fig. 9 shows that the depression waves I and II for $\epsilon = -0.01$ are expected to be separated into several waves and the depression wave III for $\epsilon = 0.01$ is expected to be separated into traveling solitary waves and the stable wave.

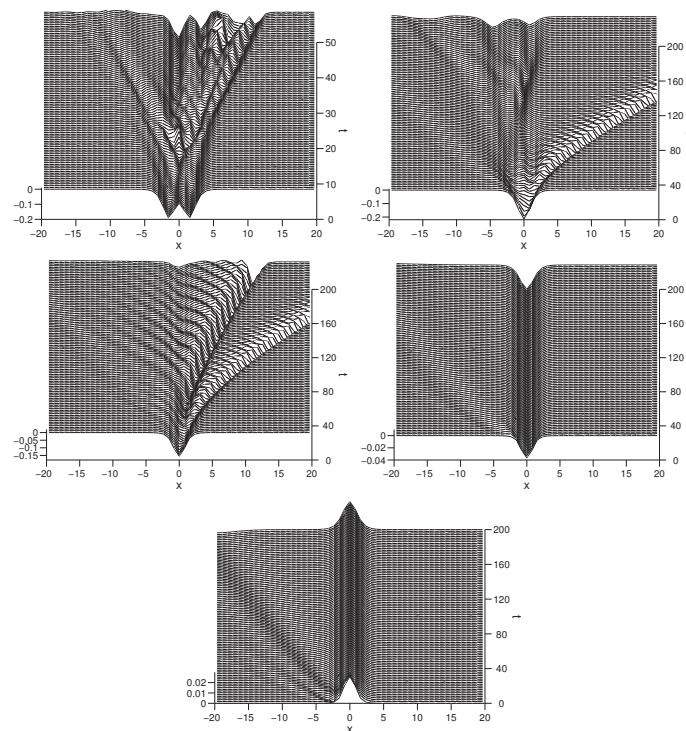


Figure 9: Means of η from (2.1) and (2.2) in time and space. Top: Depression waves I and II from $\epsilon = -0.01$, Middle: Depression waves III and IV from $\epsilon = 0.01$, Bottom: Elevation wave V from $\epsilon = -0.01$.

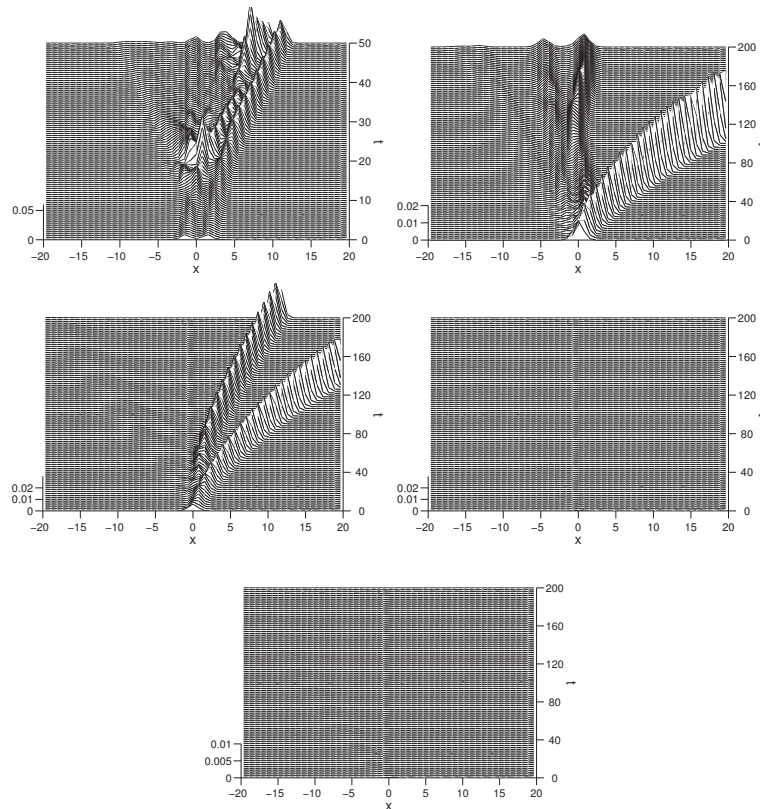


Figure 10: Variances of η from (2.1) and (2.2) in time and space. Top: Depression waves I and II from $\epsilon = -0.01$, Middle: Depression waves III and IV from $\epsilon = 0.01$, Bottom: Elevation wave V from $\epsilon = -0.01$.

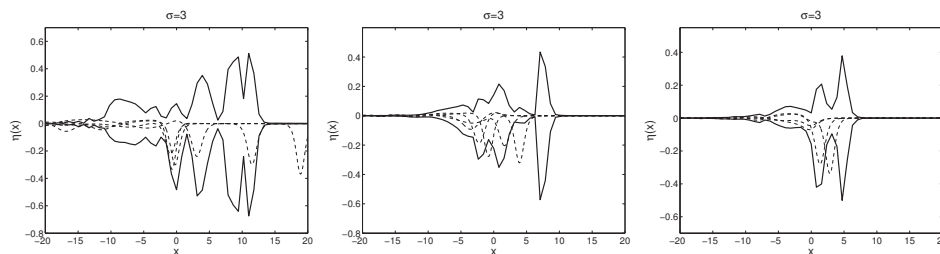


Figure 11: (Top Left) Fluctuations of the depression wave I from (2.1) and (2.2) with $\epsilon = -0.01$ for several ζ values at $t = 50$ and the curves (4.1) for $\sigma = 3$. (Top Right) Curves for the depression wave II with $\epsilon = -0.01$. (Bottom) Curves for the depression wave III with $\epsilon = 0.01$.

Fig. 11 compares the instabilities of waves I, II, III at $t = 50$ with the curves (4.1) for $\sigma = 3$ value. As in Section 4.1, the curves (4.1) seem to provide sufficient bounds for the fluctuations of unstable waves, even though curves (4.1) for smaller ζ in Figs. 7 and 8 introduce more efficient bounds.

In Sections 4.1 and 4.2, computational results for 2 uniform distributions for ζ , 3 values of σ , and 2 values of ϵ have been considered. Even though these computations are not sufficient, the results are showing that the curves (4.1) with smaller ζ and larger σ seem to encompass more fluctuations of unstable waves. $\sigma = 3$ seems to be

sufficient in the examples we considered in this study. We will study analytically and numerically on the connections among these parameters and fluctuations bounds and present the results in our future publications.

5 Conclusions

The stability of two-dimensional gravity-capillary waves has been investigated numerically based on the forced Korteweg-de Vries equation framework. The polynomial chaos method has been used to identify the stable depression and elevation wave solutions and also to estimate the magnitudes of fluctuations of unstable depression wave solutions.

More in-depth analysis of the measurements of instabilities is postponed to our future study. We will also study the effects of the random perturbations in our future research.

Acknowledgments

The authors are grateful to the anonymous referees for their valuable comments and suggestions. This research of Kim was supported by Basic Science Research Program through the National Research Foundation of Korea (NRF) funded by the Ministry of Education, Science and Technology (20110005272).

References

- [1] H. WASHIMI AND T. TANIUTI, *Propagation of ion-acoustic solitary waves of small amplitude*, Phys. Rev. Lett., 17 (1966), pp. 996–998.
- [2] T. R. AKYLAS, *On the excitation of long nonlinear water waves by moving pressure distribution*, J. Fluid Mech., 141 (1984), pp. 455–466.
- [3] R. GRIMSHAW AND N. SMYTH, *Resonant flow of a stratified fluid over topography*, J. Fluid Mech., 169 (1986), pp. 429–464.
- [4] T. Y. WU, *Generation of upstream advancing solitons by moving disturbances*, J. Fluid Mech., 184 (1987), pp. 75–99.
- [5] L. K. FORBES, *Critical free surface flow over a semicircular obstruction*, J. Eng. Math., 22 (1988), pp. 3–13.
- [6] H. SHA AND J. M. VANDEN BROECK, *Internal solitary waves with stratification in density*, J. Aust. Math. Soc. B, 38 (1997), pp. 563–580.
- [7] S. P. SHEN, R. P. MONOHAR AND L. GONG, *Stability of the lower cusped solitary waves*, J. Phys. Fluid., 7 (1995), pp. 2507–2509.
- [8] J. W. CHOI, S. M. SUN AND M. C. SHEN, *Steady capillary-gravity waves on the interface of two-layer fluid over an obstruction-forced modified k-dv equation*, J. Eng. Math., 28 (1994), pp. 193–210.
- [9] J. L. BONA, S-M. SUN AND B-Y. ZHANG, *Forced oscillations of a damped Korteweg-De Vries equation in a quarter plane*, Commun. Contemp. Math., 5(3) (2003), pp. 369–400.

- [10] N. A. LARKIN, *Modified kdv equation with a source term in a bounded domain*, Math. Methods Appl. Sci., 29(7) (2006), pp. 751–765.
- [11] J. A. PAVA AND F. M. A. NATALI, *Stability and instability of periodic travelling wave solutions for the critical korteweg-de vries and nonlinear schrödinger equations*, Phys. D Nonlinear Phenomena, 238(6) (2009), pp. 603–621.
- [12] R. CAMASSA AND T. Y-T. WU, *Stability of some stationary solutions for the forced kdv equation*, Phys. D Nonlinear Phenomena, 51(1-3) (1991), pp. 295–307.
- [13] R. CAMASSA AND T. Y-T. WU, *Stability of forced steady solitary waves*, Philos. Trans. Phys. Sci. Eng., 337(1648) (1991), pp. 429–466.
- [14] R. GRIMSHAW, M. MALEEWONG AND J. ASAVANANT, *Stability of gravity-capillary waves generated by a moving pressure disturbance in a water of finite depth*, Phys. Fluids, 21 (2009), pp. 082101-1–082101-10.
- [15] F. CHARDARD, F. DIAS, H. Y. NGUYEN AND J. VANDEN-BROECK, *Stability of some stationary solutions to the forced KdV equation with one or two bumps*, J. Eng. Math., 70 (2011), pp. 1–15.
- [16] H. KIM, W.-S. BAE AND J. CHOI, *Numerical stability of symmetric solitary-wave-like waves of a two-layer fluid-Forced modified KdV equation*, Math. Comput. Sim., 82(7) (2012), pp. 1219–1227.
- [17] M. MALEEWONG, J. ASAVANANT AND R. GRIMSHAW, *Free surface flow under gravity and surface tension due to an applied pressure distribution: I Bond number greater than one-third*, Theor. Comput. Fluid Dyn., 19(4) (2005), pp. 237–252.
- [18] R. H. CAMERON AND W. T. MARTIN, *The orthogonal development of non-linear functionals in series of fourier-hermite functionals*, Ann. Math., 48 (1947), pp. 385–392.
- [19] R. MIKULEVICIUS AND B. L. ROZOVSKII, *Linear parabolic stochastic pdes and wiener chaos*, SIAM J. Math. Anal., 29(2) (1998), pp. 452–480.
- [20] R. MIKULEVICIUS AND B. L. ROZOVSKII, *Stochastic navier-stokes equations for turbulent flows*, SIAM J. Math. Anal., 35(5) (2004), pp. 1250–1310.
- [21] R. G. GHANEM AND P. D. SPANOS, *Stochastic Finite Elements: A Spectral Approach*, Springer-Verlag, New York, 1991.
- [22] R. G. GHANEM, *Ingredients for a general purpose stochastic finite element formulation*, Comput. Methods Appl. Mech. Eng., 125 (1999), pp. 26–40.
- [23] D. XIU AND G. E. KARNIADAKIS, *The wiener-asky polynomial chaos for stochastic differential equations*, SIAM J. Sci. Comput., 24(2) (2002), pp. 619–644.
- [24] R. ASKEY AND J. WILSON, *Some basic hypergeometric polynomials that generalize Jacobi polynomials*, Mem. Amer. Math. Soc. AMS, Providence, RI, 1985.
- [25] H. KIM, *Two-step maccormack method for statistical moments of a stochastic burger's equation*, Dyn. Continuous Dis. Impulsive Syst., 14 (2007), pp. 657–684.
- [26] G. SZEGO, *Orthogonal polynomials*, American Mathematical Society, Providence, RI, 1939.
- [27] L. N. TREFETHEN, *Spectral Methods in Matlab*, SIAM, Philadelphia, PA, 2000.